China Geology 4 (2019) 512−521

China Geology

Journal homepage: http://chinageology.cgs.cn

The hydrochemical characteristics and its significance of geothermal water in both sides of large fault: Taking northern section of the Liaokao fault in north China as an example

Bao-jian Zhang[a, b,*], Tian Zhao[a, b], Yan-yan Li[a, b], Yi-fei Xing[a, b], Gui-ling Wang[c], Jun Gao[c], Xian-chun Tang[a, b], Wen-zhen Yuan[a, b], Dai-lei Zhang[a, b]

[a] *Chinese Academy of Geological Sciences，China Geological Survey, Ministry of Natural Resources, Beijing* 100037, *China*

[b] *SinoProbe Center, Chinese Academy of Geological Sciences, China Geological Survey, Ministry of Natural Resources, Beijing* 100037, *China*

[c] *Institute of Hydrogeology and Environmental Geology, Chinese Academy of Geological Sciences, China Geological Survey, Ministry of Natural Resources, Shijiazhuang* 050061, *China*

ARTICLE INFO

Article history:
Received 14 September 2019
Received in revised form 21 October 2019
Accepted 12 November 2019
Available online 24 December 2019

Keywords:
Geothermal survey engineering
Large-scale fault
Hydrochemistry
Geothermal water
Zonal characteristics
Indicative meaning
Liaokao fault
North China

ABSTRACT

Based on comparative analysis on hydrochemical characteristics of geothermal water in the north part of Liaokao fault, this research focuses on studying the indicative significance of hydrochemical characteristics for the formation of geothermal water. The result shows that: (1) There is no obvious hydraulic connection between the karst geothermal water (occurred in the east part of the Liaokao fault) and the sandstone geothermal water (occurred in the west part of Liaokao fault). (2) In a close hydrological environment, caused by tectonic activities, geothermal water remains longer time in reservoir, hence the water-rock interaction is more complete, with high degree of concentrations, whereas the renewable capacity of the water is weaker. (3) There is no high temperature mantle source fluid mixed in the geothermal water. Karst geothermal water occurred deep circulatory convection along Liaokao fault and its secondary fault, therefore there is deep crust source fluid added into the geothermal water, closer to the Liaokao fault, the greater affected by the deep crust fluid. However, sandstone geothermal water has weak deep circulatory convection.

1. Introduction

According the geological environment and heat transfer way, Muffler LJP (1976) proposed that the geothermal can be divided into convective and conductive types. Combined with structural factors, Tian TS et al. (2006) classified the Chinese geothermal reservoir into two types, i.e., sedimentary basin conductive geothermal reservoirs and uplifted mountain faults convective. Zhang Y et al. (2017) deemed that adequate water supply and fault development are the main controlling factors for the formation of uplifted mountain hydrothermal geothermal system. Large-scale high-quality reservoirs with certain depth are the main controlling factors for the formation of hydrothermal geothermal system in sedimentary basins. Pang ZH et al. (2017) pointed out that the heat transfer method of geothermal resources in Xiongan New Area is mainly conductive in the Cenozoic caprock, and is convective in the bedrock reservoir, which assigns to the "convection-conducting geothermal system".

China has entered an age of rapid development of geothermal energy since 2010, and the exploring depth of geothermal water is continuously increasing (Violay M et al., 2017; Wang GL et al., 2018). Some geothermal researchers have recognized the controlling effect of fault structure on the formation of geothermal resources (Zhao YJ et al., 2016), and analyzed the nearby geothermal resources including the characteristics, genesis and water and heat conduction of faults (Tang XC et al., 2017; Feng YF et al., 2018; Liu J et al., 2018; Xu P et al., 2018; Rosberg JE and Erlstrom M, 2019). Zhang BJ et al. (2010) and Yu J et al. (2013) respectively speculated the existence of hidden faults by the hydrochemistry and temperature anomalies of the geothermal water. Du GL et al. (2012) pointed out that the weakening effect of the water deep cycle of Baoquantang hot spring in Weihai City and the release of thermal energy from hot springs reduced the fault and seismic activity in this area. According to the hydro-chemical anomaly of geothermal water near the fault, Zhang BJ et al. (2010) proposed a type of noteworthy conceptual model of geothermal resources, named

* Corresponding author: *E-mail address*: zbjsddk@126.com (Bao-jian Zhang).

doi:10.31035/cg2018132
2096-5192/© 2019 China Geology Editorial Office.

"tectonic trap geothermal resources" (Zhang BJ et al., 2009a).

The Liaokao fault is a large-scale deep fault in the southeastern margin of the North China. Previous research shows that the Liaokao fault and its secondary faults have an obvious control effect on the formation of geothermal resources (Zhang BJ, 2009b). Based on the previous research, this paper further analyzes the characteristics and differences of geothermal water hydration zones of different heat storage types on both sides of the northern section of the Liaokao fault, and expounds its indicating significance.

2. Thermal reservoir and geological background

2.1. Geological background

The Liaokao fault, the boundary fault of the Huabei depression and Luxi land, extend from Lankao of Henan province to north Liaocheng of Shandong province, and has wide fracture intersection with Qiguang fault. The northern part of Liaokao fault in Shandong province is mainly located in Liaocheng and Heze. In Liaocheng section, the west side is Shenxian sag of the Linqing depression and the east side is Yanggu-Qihe convex of the Luzhong uplift. The west side of Heze section is Dongming sag of Linqing depression, and the east side is Heze convex of Luzhong uplift (Fig. 1).

The Liaokao normal fault rises in the east and falls in the west. The Liaokao fault controls the development of the western depression and the eastern uplift as the Mesozoic strong tectonic activities and continuing to be active during Neogene, until to Quaternary. Since 953 AD, Liaokao fault happened 15 times earthquake which is near 5 magnitude above. It shows that the fault is an active neotectonic active belt (Wang XC et al., 2001). The multi-stage fault activities make the fault interval huge, with the maximum fault interval reaching 5600 m in Liaocheng and 7200 m in Heze, which has obvious control effect on the strata (Wang MJ et al., 2011). Carboniferous Permian or Ordovician is directly covered by the Neogene in uplift side of central Luzhong uplift. The descending side is deposited Mesozoic and Cenozoic strata about several kilometers thick (Fig.1).

2.2. Main thermal reservoir

According to the existing geothermal well data, there are 3 main thermal reservoirs that can be utilized in the study area, namely, the crevice-pore type of sandstone in the Neogene Guantao formation, the Paleogene Dongying formation and the crevice-karst type of limestone in the Cambrian Ordovician. This study focuses on the karst geothermal field in the east of Liaocheng, the Heze convex karst geothermal field, the Liaocheng west sandstone geothermal field and Dongming sandstone geothermal field in the west of the Liaokao fault.

(i) Guantao Formation thermal reservoir: It is mainly distributed to the west of Liaokao fault. The buried depth of the top plate of the thermal reservoir is 950−1000 m, and that of the bottom plate is 1250−1800 m. The buried depth in Heze is slightly larger than that in Liaocheng. The lithology is medium-fine, medium-coarse sandstone, pebbly medium coarse sandstone, silty sand and mudstone interbeds. Medium-fine, medium-coarse sandstone and pebbly medium coarse sandstone are good aquifers, and single well water inflow is 1000−1500 m^3/d. The water temperature is 50−60℃.To the east of the Liaokao fault, Guantao formation is not fully developed. The buried depth of the floor is generally less than 1000 m and the water temperature is relatively low, so it is generally not exploited as an independent thermal reservoir.

(ii) Dongying Formation thermal reservoir: It is only distributed to the west of Liaokao fault. The buried depth of the top plate of the thermal reservoir is 1250−1800 m, and the predicted buried depth of the bottom plate is 1700−2100 m. The lithology is medium-fine, medium-coarse, coarse sandstone, silty sand and mudstone interbed. The single well water inflow is 1500−2000 m^3/d, the water temperature 55−70℃.

(iii) Cambrian-Ordovician thermal reservoir: It is distributed in the uplift area in the east of Liaokao fault. The Guqian hill's top Ordovician thermal reservoir roof is buried at a depth of 800−1000 m, and the Guqian hill 's edge Ordovician thermal reservoir roof is buried at a depth of about 1200 m. The lithology is mainly thick layer limestone and leopard skin limestone, fracture and karst is developed. The buried depth of the Cambrian thermal reservoir roof is about

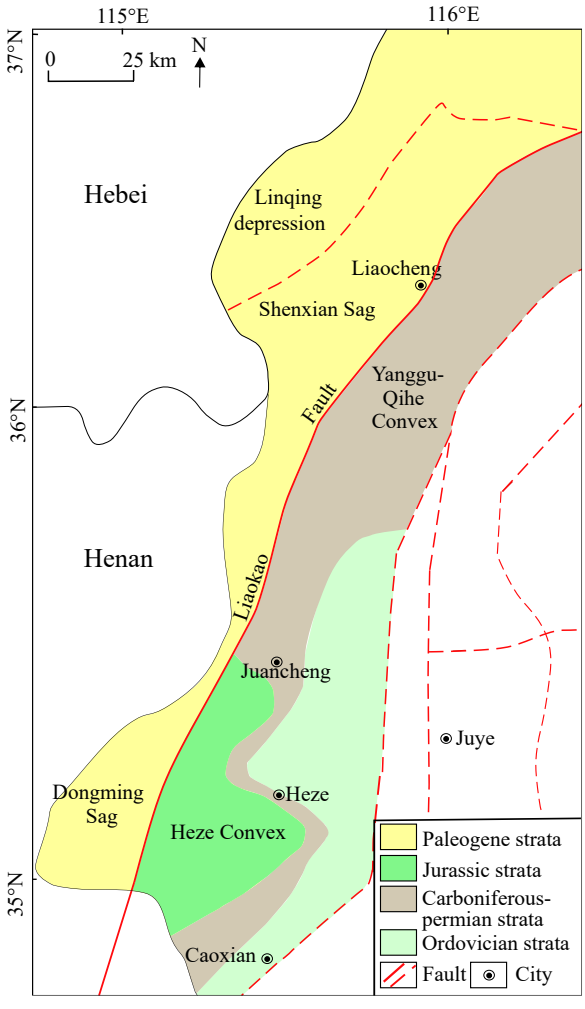

Fig. 1. Regional Pre-Neogene basement rock geological map in the northern section of the Liaokao fault, north China.

1700 m. The hot water mainly occurs in the karst fissures of layered limestone. The thermal reservoir aquifer is dominated by old dissolution zone of the thick crystalline secondary limestone in upper Ordovician limestone. The flow automatically rate is 400−1000 m^3/d, wellhead temperature is 53−68℃.

3. Geochemical characteristics of geothermal fluid from both sides of Liaokao fault

3.1. Samples and study methods

A total of 25 water samples from study area were collected for major iron chemistry, and 17 water samples for δD and $\delta^{18}O$, 16 for T, 12 for ^{14}C and ^{13}C, as well as 8 for ^{3}He, ^{4}He, ^{20}Ne. While sampling, all water samples were filtered through 0.45 μm membranes on site. Samples were stored in new 350 mL polyethylene bottles that were rinsed with deionized water twice before sampling.

The chemical analysis of the major anions and cations was conducted in the North Shandong Geological Engineering Investigation Institute and the results are showed in Table1. Na^+, K^+, Ca^{2+}, were determined with an atomic absorption spectrophotometer. Cl^- and HCO_3^- were determined volumetrically. The anion-cation balance check is based on the percentage difference between total positive charge and total negative charge. Isotope analysis was carried out at the Beijing Nuclear Industry Research Institute, and the results are showed in Table1. Samples for δD and $\delta^{18}O$ analysis were analyzed using an isoprime Dual Inlet Isotope Ratio Mass Spectrometer (DI-IRMS) coupled to a multiprep bench for online analysis. δD was analyzed for after online equilibration at 40℃ with a platinum catalyst (Hokko beads). $\delta^{18}O$ were analyzed as above, but after equilibration with carbon dioxide. The δD and $\delta^{18}O$ conformed to the international water standards of IAEA and USGS and were determined with a precision below ±2‰ for δD and ±0.1‰ for $\delta^{18}O$. In addition, the Deuterium (d) excess value was calculated with the

Table 1. Comparison of geothermal water quality of each section in Liaocheng.

Component classification		The west section of Liaokao fault				The east section of Liaokao fault	
		Sandstone geothermal water of geothermal field in Dongming		Sandstone geothermal water of geothermal field in the West of Liaocheng		Karst geothermal water of geothermal field in the East of Liaocheng	Karst geothermal water of geothermal field of Heze convex
		Non-trap type	Trap type	Non-trap type	Trap type		
Key component (mg/L)	K^+	5.8−15.3	26.1−35.4	2.03−13.43	29.85−37.75	59.25−66.5	5.83−42.2
	Na^+	943−977	2538−3986	501−1658	2801−4068	726−812	393−538
	Ca^{2+}	28−192	397−679.4	66−278	432−607	677−707	471−533
	Mg^{2+}	8.51−23.09	89.3−123.93	31.59−72.13	98.3−138.5	154.3−173.8	93−137
	Cl^-	783−840	3846−7285	350.96−1858	4405−6576	1514−1631	323−499
	SO_4^{2-}	581−1285	780−1105	708−1911	1105−1790	1599−1729	1739−2224
	HCO_3^-	189−378	104−201	140−275	73−155	171−177	65−174
Trace component (mg/L)	F^-	0.75−1.25	0.5−2.12	0.25−1.8	0.75−1.5	3.25−3.5	1.3−3.5
	I^-	0.52−0.6	1.3−1.92	0.25−1.45	3−5.5	<0.10−0.11	<0.10−1.9
	Br^-	1.2−1.3	9.6−12.0	1.2−3	2.4−19.2	1.7−3.5	0.6−3.2
	Sr^{2+}	0.6−2.7	14.7−24.9	0.6−7.5	16.9−22.3	12.8−14.2	4.9−10.7
	Li^-	0.19−0.57	0.36−0.56	0.15−0.9	0.39−0.49	1.28−1.4	0.1−1.03
	$HSiO_3^-$	42.25	35.75−42.25	22.75−39	35−35.75	35.75−45.5	25.2−48
Characteristic coefficient	rNa^+/rCl^-	1.73−1.92	0.84−1.02	1.38−2.2	0.92−1.11	0.70−0.77	1.47−3.94
	$(100\times rSO_4^{2-})/rCl^-$	51.2−121.3	7.92−21.24	58.24−149.3	14−30	75.4−79.5	258−506
	$rC1^-/(rHCO_3^-+ r\,CO_3^{2-})$	3.8−7.1	32.8−120.7	2.20−19.1	48.8−154.3	14.7−16.4	3.20−8.59
Isotope	^{14}C age/10^4a	0.70−0.96		0.31−0.98		1.53−3.45	0.16−1.35
	$d=\delta D-8\delta^{18}O$	–2.7	–6.4	–6.7−1.3	–5.5−–9.2	1.7−4	–0.5−4.1
	$R=^3He/^4He/\times10^{-7}$	2.64−2.92		1.25−1.81		0.97−1.25	3.20
	R/Ra	0.19−0.21		0.09−0.13		0.07−0.09	0.23
	$^4He/^{20}Ne$	411−437		50−925		1242−1296	381−417
Helium isotope source	Atmospheric source/%	18.17−20.19		8.07−12.11		6.05−8.07	22.21
	Crustal source/%	79.81−81.83		87.89−91.93		91.93−93.95	77.79
Other parameters	Salinity/(mg/L)	2820.81−3503.67	8282.95−13010.09	1969.66−5487.54	9418.29−12775.25	4965.76−5229.56	2040.84−4111
	Total hardness /(mg/L)	105.08−575.46	1501.2−2064.15	350.28−990.89	1496.61−2001.6	2391.9−2416.93	105.08−1851
	pH	7.5	7.1−7.4	7.4−8.1	7.0−7.2	7.0−7.1	7.0−7.4
	Hydrochemical types	SO_4·Cl-Na、Cl·SO_4-Na	Cl-Na	SO_4·Cl-Na、Cl·SO_4-Na	Cl-Na	Cl·SO_4-Na Ca、Cl·SO_4- Ca Na	SO_4- Ca Na、SO_4-Na Ca

formula δ=δD–(8δ^{18}O) using the δ^{18}O and δD isotope results. The helium ratios were measured using Noblesse Mass Spectrometry.

3.2. System on hydrochemical evaluation of geothermal fluid.

The content of various ions, the ratio between different ions, isotopic composition and gas composition in water are the most commonly used indicators in the analysis of the formation environment of geothermal water. According to the hydrochemistry test project of geothermal water and the basis of previous studies, the following evaluation indexes and their combination were selected to analyze and study the difference of the hydration zone of geothermal water in the northern section of the Liaokao fault.

(i) Main components, salinity and hydrochemical types of geothermal water. Generally, the circulating runoff conditions of groundwater gradually deteriorate from the recharge area through the runoff area to the formation area of geothermal water. The degree of water-rock interaction gradually increases. It is gradually increased to dissolve surrounding rock composition, and the salinity gradually increases. The main anion evolution direction in water is: HCO_3^-→SO_4^{2-}→Cl^-; On the other hand, the main kation evolution direction is: Ca^{2+}, Mg^{2+}→Na^+, Ca^{2+}. In addition, the composition of geothermal water varies greatly due to the types of rocks, thermal reservoirs and surrounding rocks through which geothermal water flows.

(ii) Trace components of geothermal water. In general, the content of most trace elements in geothermal water is generally higher than that in cold water. The content of most trace elements increased gradually from the recharge area through the runoff area to the formation area of geothermal water. The types of rock, reservoir and surrounding rock through which geothermal water flows are also important limiting factors for the difference of trace components of geothermal water.

(iii) Mineral Saturation Index. According to the equilibrium diagram of geothermal water Na-K-Mg (Fig. 2), the geothermal water in the study area falls into the non-equilibrium zone and the basic equilibrium zone (and is close to the non-equilibrium zone), indicating that the water-rock interaction has not reached the equilibrium state and the dissolution is still in progress. PHREEQC software was used to calculate the mineral phase equilibrium of geothermal water in the study area, and the saturation index (*SI*) of various minerals in the water sample was obtained (Table 2) by using the software. It can be concluded from Table 2 that the soluble components such as rock salt, gypsum and anhydrite are not saturated in geothermal water in the main mineral components of heat storage and surrounding rocks in the study area, while the insoluble components such as calcite, aragonite, dolomite, quartz, chalcedony and talc are basically saturated. The difference of the soluble components *SI* reflects not only the difference of thermal reservoir lithology but also the difference of geothermal water circulation conditions.

(iv) Ratio Ions (Characteristic Coefficient). Based on the fixed relationship between the contents of some elements, the causes of groundwater and its environment can be analyzed and judged. For example, sodium chloride coefficient (rNa$^+$/rC1$^-$), desulfurization coefficient (100×rSO$_4^{2-}$ / rC1$^-$), salinization coefficient [rC1$^-$/ (rHCO$_3^-$+rCO$_3^{2-}$)] (Chen ZH et al., 2012).

The sodium-chlorine coefficient reflects the degree of formation water concentration and metamorphism and the hydro-geochemical environment of the reservoir. It is known that the smaller the sodium-chlorine coefficient is, the better the formation water is closed. What 's more, the more concentrated it is, and the deeper the metamorphism is, which is reflected to be similar with relatively hydrological environment. Except for the karst geothermal field in the east of Liaocheng which is slightly less than 0.85 (the ratio of sodium-chlorine coefficient of seawater), other the hot fields and hot water in the study area are slightly higher than 0.85, indicating that the geothermal water is affected by the infiltration water, and the higher the sodium-chlorine coefficient, the stronger the infiltration water activity.

The desulfurization coefficient indicates the redox environment of formation water. It is generally believed that the smaller the desulfurization coefficient is, the better the formation water sealing is. The formation water with a desulfurization coefficient which is less than 1 usually indicates that the formation water has been thoroughly reduced and buried in a well-sealed area. On the contrary, it is believed that the reduction is not complete and may be affected by superficial oxidation. The desulfurization coefficient of geothermal water in all areas of the study area is much higher than 1, which indicates that they are obviously affected by superficial oxidation.

The salinization coefficient mainly reflects the concentration of formation water. The higher the salinization coefficient is, the higher the salinity of formation water is and the higher the concentration of formation water is.

(v) Isotopes. δD, δ^{18}O, ^{3}H (Tritium), ^{14}C, ^{3}He/^{4}He,

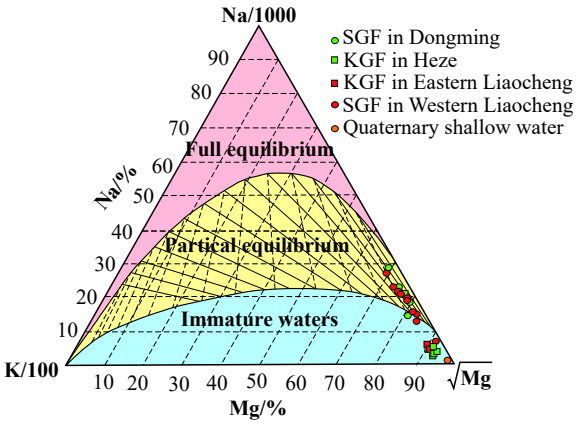

Fig. 2. Equilibrium diagram of Na-K-Mg in geothermal water on both sides of north section of Liaokao fault. SGF−sandstone geothermal field; KGF−Karst geothermal field (After Giggenbach, 1988).

Table 2. Statistical table of main mineral saturation index (*SI*) of geothermal water calculated by PHREEQC software in the Heze, Liaocheng.

Mineral name	Molecular formula	Saturation index statistics	Sandstone geothermal water of geothermal field in Dongming	Karst geothermal water of geothermal field of Heze convex	Sandstone geothermal water of geothermal field in the West of Liaocheng	Karst geothermal water of geothermal field in the East of Liaocheng
		Sample number	4	6	10	3
Anhydrite	$CaSO_4$	value range	−1.67−−0.57	−1.48−−0.06	−1.12−−0.41	−0.11−−0.13
		mean	−0.89	−0.35	−0.62	−0.12
Aragonite	$CaCO_3$	value range	−0.06−0.48	−0.22−0.51	0.10−0.96	0.39−0.53
		mean	0.33	0.19	0.41	0.45
Calcite	$CaCO_3$	value range	0.06−0.71	−0.09−0.63	0.23−1.09	0.51−0.65
		mean	0.45	0.31	0.54	0.57
Dolomite	$CaMg(CO_3)_2$	value range	0.08−2.04	−0.35−0.97	0.14−1.88	0.79−1.14
		mean	0.90	0.35	0.91	0.94
Gypsum	$CaSO_4{\cdot}2H_2O$	value range	−1.62−−0.59	−1.39−−0.08	−1.14−−0.40	−0.15−−0.11
		mean	−0.91	−0.32	−0.58	−0.14
Halite	NaCl	value range	−4.89−−3.84	−5.67−−5.42	−5.49−−3.42	−4.76−−4.69
		mean	−4.50	−5.56	−4.24	−4.73
Celestine	$SrSO_4$	value range	−1.52−−0.23	−1.68−0.01	−1.40−0.10	−0.06−−0.03
		mean	−0.71	−0.39	−0.39	−0.05
Strontianite	$SrCO_3$	value range	−1.26−−0.39	−1.62−−0.73	−1.10−−0.54	−0.89−−0.72
		mean	−0.81	−1.19	−0.70	−0.81
Fluorite	CaF_2	value range	−2.31−−0.61	−1.18−0.13	−2.93−−0.74	0.03−0.05
		mean	−1.60	−0.32	−1.30	0.04
Chalcedony	SiO_2	value range	−0.02−0.12	−0.13−0.14	−0.24−0.13	−0.03−0.09
		mean	0.04	−0.02	0.01	0.03
Chrysotile	$Mg_3Si_2O_5(OH)_4$	value range	−2.43−4.62	−2.69−−1.14	−1.67−1.54	−1.25−−0.48
		mean	0.11	−1.78	−0.01	−0.85
Quartz	SiO_2	value range	0.29−0.48	0.22−0.49	0.09−0.49	0.30−0.43
		mean	0.37	0.33	0.36	0.36
Talc	$Mg_3Si_4O_{10}(OH)_2$	value range	1.82−8.75	0.32−3.04	2.90−6.93	3.01−3.56
		mean	4.27	1.96	4.04	3.30

$^4He/^{20}Ne$ are usually used to trace the environmental information for the formation of geothermal water.

The δD versus $\delta^{18}O$ diagram indicates that the source of geothermal water supply, hydraulic contact and supply elevation. The quaternary shallow water, the deep water of the Minghuazhen formation and the geothermal water in different places in the study area all fall near the right side of the global rain water line (GMWL of Craig) and the rain water line in Jinan in Fig. 3 (Yang LZ et al., 2009). It indicates that the recharge sources of all types water bodies in the area are meteoric precipitation. The $\delta^{18}O$ has significant right drift indicating the geothermal water occurred in a closed tectonic environment, caused by the complete water-rock interaction (Craig, 1963; Ma ZY et al., 2008). The values of δD and $\delta^{18}O$ in the geothermal water are generally lower than that in the local quaternary shallow cold water. Therefore, it is inferred that the supply source should be the precipitation infiltration from the higher elevation or in a cold period.

^2H excess parameter d ($d=\delta D-8\delta^{18}O$) is commonly used to evaluate the renewable capacity of geothermal water (Ma ZY et al., 2004), and d can be used as a measure of ^{18}O isotope exchange degree in water-rock interaction. The smaller the d value is, the more closed the hydrogeological environment is, the longer the water will remain in the aquifer, the slower the groundwater runoff will speed and the weaker the renewable capacity of geothermal water is.

The half-life of ^{14}C is 5730±40 a, so it is suitable for studying the deep and older groundwater. The geothermal fluid in the study area is buried deep and old, so the determination of geothermal water age using ^{14}C is much more accurate.

The difference in $^3He/^4He$ ratio can distinguish whether there is upwelling deep mantle source fluid with high heat in geothermal water, and the relationship between $^3He/^4He$ and $^4He/^{20}Ne$ can distinguish the influence the degree of geothermal water on atmospheric helium, crustal helium and mantle helium. It can provide the evidence for the study of the genesis of geothermal water (Sun ZX et al., 2014. Luo L et al., 2014). The R/Ra ratio of all geothermal water sample points in the study area is less than 1 (Table 2), indicating that helium in geothermal water is mainly caused by shell source helium, and there is basically no deep mantle source fluid. For the Fig. 4 all the geothermal water points is in the triangle area that is composed of end elements about atmosphere (A)/mantle (B) and lithosphere (C) and belongs to the one side of the atmosphere and the crust. Therefore, the sources of the helium gas in geothermal water are mainly from the mixture of atmospheric helium and shell source of helium,

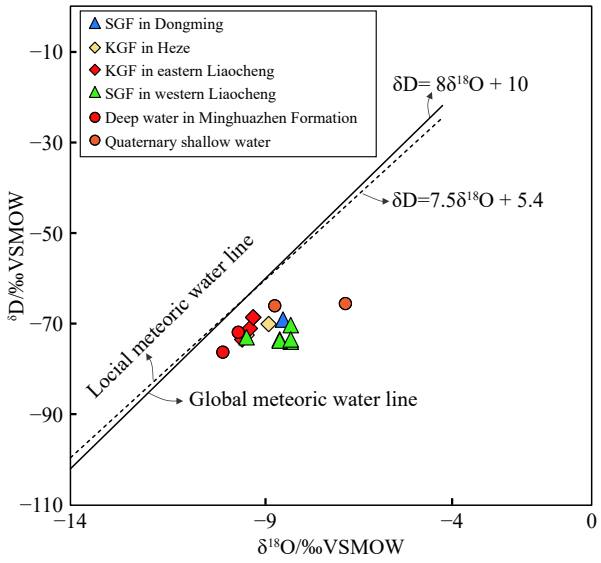

Fig. 3. Plot of δD vs. δ^{18}O for the geothermal water of northern Liaokao fault. Global meteoric water line is from Craig (1961) and local meteoric water line is from Yang et al. (2009). SGF−Sandstone geothermal field; KGF−Karst geothermal field.

and given priority to with the source of the shell source helium. All these results indicate that the geothermal water is derived or mixed with mantle fluid.

In view of the fact that the helium isotopes in the geothermal water in the study area are mainly from the large gas source and crustal source, and there is almost no mantle-source helium mixing, which belongs to binary mixing. In order to understand the contribution of helium isotopes in the atmosphere and crust to the geothermal water in the region, the binary mixing model was used to quantify the source of helium isotopes. The specific calculation formula is shown in equation 1. In formula 1:X is the proportion of end elements mixed with A; 1-X is the proportion of C-terminal elements mixed in; (^{3}He/^{4}He) A and (^{3}He/^{4}He) C are respectively the helium isotope ratios of terminal element A and terminal element C. (^{3}He/^{4}He) M is the helium isotope ratio of the sampling point. The calculation results are shown in Table 2.

$$\left(^3\mathrm{He}/^4\mathrm{He}\right)\mathrm{M} = \mathrm{X} * \left(^3\mathrm{He}/^4\mathrm{He}\right)\mathrm{A} + (1-\mathrm{X}) * \left(^3\mathrm{He}/^4\mathrm{He}\right)\mathrm{C} \quad (1)$$

3.3. Difference on carbonate rocks karst geothermal fluid

The salinity of karst geothermal water in East Liaocheng is about 1 g/L higher than that of Heze uplift (Fig. 5). The hydro-chemical types of karst geothermal water in East Liaocheng are mainly Cl·SO_4-Na·Ca, Cl·SO_4-Ca·Na, and the anions are mainly Cl^- and SO_4^{2-}.The hydro-chemical types of Heze convex geothermal water are mainly SO_4-Ca·Na, SO_4-Na·Ca, and the anions are mainly SO_4^{2-}.In the chemical water Piper three chart (Fig. 6), East Liaocheng karst geothermal water (Ⅲ area) is on the right of the Heze bump (Ⅱ area). In Na-K-Mg equilibrium graph (Fig. 2), East Liaocheng karst geothermal water is closer to local equilibrium than Heze convex.

The sodium chloride coefficient and the desulfurization coefficient in the East Liaocheng karst geothermal water are significantly lower than the Heze. The salinization coefficient is significantly higher than the Heze convex. The saturation index of halite, gypsum and anhydrite, aragonite and calcite, dolomite, lapis lazuli, strontium ore is obviously higher than that of Heze. The proportion of ^{14}C age and shell source helium is significantly higher than Heze uplift. This indicates that the hydrological environment of the karst geothermal field in the east of Liaocheng is more closed with stronger reducibility, more complete water-rock interaction and higher concentration. The reason is that the karst geothermal field in the east of Liaocheng is small; the Ordovician thermal reservoir is butted with the Neogene sand and mudstone in the west, and is butted with the carboniferous and Permian with poor permeability in the north, east and south, so the hydrological environment is more closed. The Ordovician thermal storage area of Heze uplift is large, and the northeast part of it is affected by the recharge of large area shallow buried karst water (buried depth less than 700 m). The ^{14}C value of the karst geothermal water in the east of Liaocheng is obviously higher than the ratio of shell source helium. The reason may be the geothermal water is closer to the Liaokao fault, so the geothermal water circulates deeper along the Liaokao fault and is more affected by the deep materials.

3.4. Difference between trap and non-trap sandstone reservoirs

Previous research results have found that there are structural trap geothermal resources with abnormally high salinity in the West Liaocheng sandstone geothermal field on the west side of the Liaokao fault (Zhang BJ et al., 2009a). This type of structural trap geothermal resource is formed by the connection between sandstone thermal storage and cement rock due to the dislocation of faults. Besides the similar trap geothermal water has been found in the Dongming geothermal field (Fig. 5).

The trap geothermal water salinity which is close to the buried depth in the western Liaocheng geothermal field is 4−8 g/L higher than that of the non-trap geothermal field, and

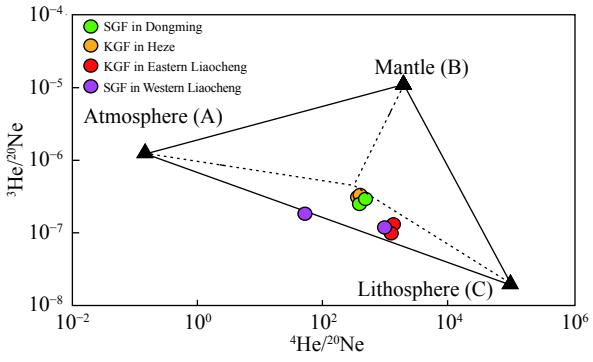

Fig. 4. Plot of ^{3}He/^{20}Ne vs. ^{4}He/^{20}Ne for the geothermal water of northern Liaokao fault (After Stuart et al., 1995).

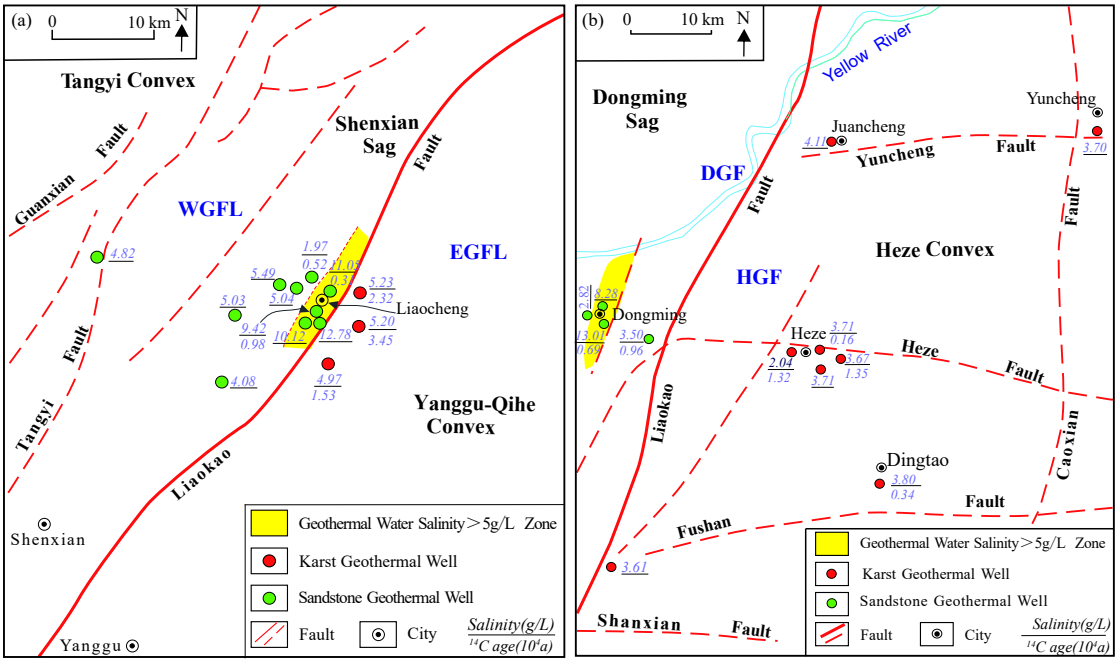

Fig. 5. Distribution of salinity and ^{14}C for the geothermal water of northern Liaokao fault. EGFL−East Geothermal Field of Liaocheng; HGF−Heze Geothermal Field; DGF−Dongming Geothermal Field; WGFL−West Geothermal Field of Liaocheng.

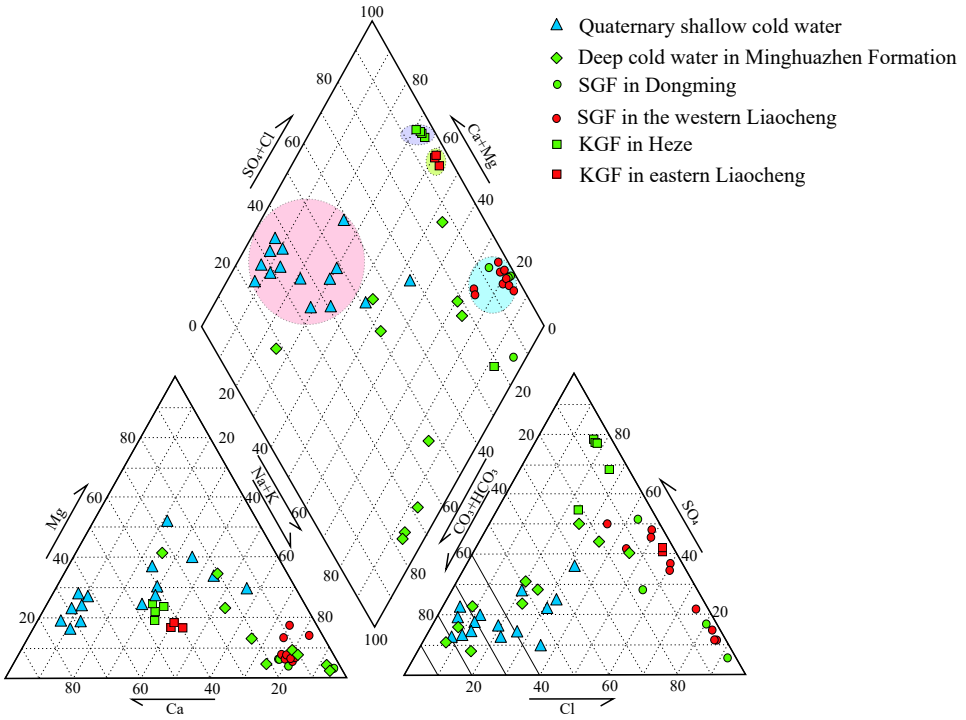

Fig. 6. The Piper tri-graph of hydrochemistry of geothermal water on both sides of the northern section of the fault. SGF-Sandstone geothermal field; KGF-Karst geothermal field.

the trap geothermal water salinity which is close to the buried depth in the Dongming geothermal field is 5−10 g/L higher than that of the non-trap geothermal field (Fig. 5).The hydrochemical type of trap sandstone geothermal water is Cl-Na type, and the anions are mainly Cl^-.The hydro-chemical types of non-confined sandstone geothermal water are mainly SO_4·Cl-Na, Cl·SO_4-Na, and the anions are mainly Cl^- and SO_4^{2-}. The contents of trace elements I^-, Br^-, Sr^{2+} in trap sandstone geothermal water are significantly higher than those in non-trap type, which indicates that the more closed the hydrological environment is, the longer the hot water retention time is, and the more these trace elements are dissolved. The saturation indexes of Lapis lazuli and strontiumite in geothermal water are both negative, indicating that the dissolution continues.

The sodium-chlorine coefficient and desulfurization

coefficient of trap type sandstone geothermal water is significantly lower than those of non-trap type, however the salinization coefficient was significantly higher than that of non-trap type, but there is no significant difference between ^{14}C age and the ratio of shell source helium. It indicates that the recharge source and recharge time of sandstone geothermal water in the study area are basically the same, but the hydrological environment of trap geothermal water is more closed with stronger reducibility, more complete water-rock interaction and higher concentration. The excess parameter *d* value of ^{2}H of trap geothermal water is slightly smaller than that of non-trap geothermal water, indicating that the hydrogeological environment of trap geothermal water is more closed, and the water stays in the aquifer is longer, and the groundwater runoff speed is slower, and the renewable capacity of geothermal water is weaker.

3.5. Difference between carbonate-rock and sandstone reservoirs

The mineralization of karst geothermal water in the eastern part of the Liaokao fault is slightly higher than or equal to that of non-trap sandstone geothermal water in the western part of the fault, while it is obviously lower than that of trap sandstone geothermal water (Fig. 5 and Table 1). The content of Ca^{2+}, Mg^{2+}, K^{+} and total hardness of karst geothermal water are significantly higher than that of sandstone geothermal water, and the contents of Na^{+}, Cl^{-}, I^{-} of sandstone geothermal water were significantly higher than that of karst geothermal water. The saturation index of gypsum, anhydrite and lapis lazuli of karst geothermal water is obviously higher than that of sandstone geothermal water, and the saturation index of sandstone geothermal water and rock salt is obviously higher than that of karst geothermal water. This reflects that the obvious difference of hydrochemistry of geothermal water is caused by the different lithology of thermal reservoir.

The content of F^{-}, Li^{-}, Sr^{2+} in karst geothermal water is obviously higher than that in sandstone geothermal water. The F^{-} content of karst geothermal water is relatively high. The reasons as follows: Firstly, the bottom of the Cambrian-Ordovician is the Archean erathem Angle of biotite granite and gneiss. And fluorine content is higher in the biotite and hornblende. Biotite amphibolite and gneiss in the lower part of long-term are leached by the heat storage of deep circulating geothermal water which fluoride salts and fluorosilicate minerals are dissolved and hydrolyzed; Secondly, the Ordovician limestone and dolomite paste salt content is large, and often has gypsum interlayer, due to the dissolution of gypsum, it can result in the increase of calcium ions in water, and in the precipitation of HCO_3^{-} and Ca^{2+} to calcium carbonate, and promote the dissolution of fluorite.

The reason for the high Li^{-} content may be that the Archean biotite amphibolite granite and gneiss in the lower part of the Cambrian-Ordovician in the study area contain more biotite, and biotite is the main mineral that concentrates and carries lithium. Therefore, the content of lithium in karst geothermal water is relatively higher. The content of Sr^{2+} is relatively higher, which may be due to 3 reasons. Firstly, the main minerals containing strontium in nature (such as celestine) are mainly produced in dolomite, limestone and other carbonate rocks, but are relatively scarce in sand and mudstone. The other reason is that due to the high content of Ca^{2+} in karst water and dolomitization, the concentration of HCO_3^{-} and Sr^{2+} are in a reciprocal relationship. With the concentration of HCO_3^{-} decreasing, the content of Sr^{2+} increases. The third reason is that the concentration of Sr^{2+} is positively correlated with the concentration of SO_4^{2-}. With the concentration of SO_4^{2-} increasing, the solubility of strontium-containing minerals increases.

The ^{14}C value of karst geothermal water in the eastern part of the fault is slightly higher than that of sandstone geothermal water in the western part of the fault, while the excess parameter *d* value of ^{2}H is obviously higher than that of sandstone geothermal water. This shows that although water runoff is faster and renewable ability is stronger in karst geothermal. But due to the major fault and its secondary fault and other large fracture existing, the karst geothermal water flows along the fracture to the deep circulation convection and obtains higher age. Compared with the geothermal water, the karst sandstone geothermal water convectional circulation phenomenon is very weak or nonexistent. The oxygen drift of sandstone geothermal water is more obvious than that of karst geothermal water (Fig. 3), indicating that the recharge distance of sandstone geothermal water is farther, and there should be precipitation recharge from the western Taihang Mountains.

4. Significance of zonal difference of geothermal water

4.1. Hydraulic relationship between geothermal water of different types on both sides of the Liaokao Fault

According to the survey about examination, the karst fracture head height on the east side of geothermal water is higher than that of the west of the sandstone type of pore water head height about 8−15 m. The karst geothermal water supply on the hydrodynamic conditions have on the east side to the west of the sandstone geothermal water conditions, but the geothermal water on both sides of the fracture is significantly different in terms of major component, trace component, ^{14}C value, and excess parameter *d* value at ^{2}H. It shows no apparent connection between them.

This test is located in Heze uplift of farce eagle geothermal well is to use the Guantao sandstone and the Ordovician karst geothermal water mixed water. The salinity is 2 g/L, and hydro-chemical type is SO_4-Na, including Na^{+}, Ca^{2+}, Mg^{2+}, Cl^{-}, SO_4^{2-}, HCO_3^{-} content respectively: 597 mg/L, 34 mg/L, 4.86 mg/L, 234 mg/L, 749 mg/L, 390 mg/L. It is obviously different from Liaokao fracture on the east side of the fracture karst geothermal water, also is very different from Liaokao fracture on the west side of sandstone geothermal water (Table 1). From the perspective of hydrochemistry, it is

shown that there is no obvious hydraulic relationship between the karst geothermal water on the east side of the Liaokao fault and the west side.

However, there are residual Guantao formation and Minghuazhen formation sandstone thermal reservoirs on the top of the karst thermal reservoir on the east side of the Liaokao fault, which can supply the geothermal water of the sandstone on the west side of the Liaokao fault.

4.2. Difference on hydrothermal environment and characteristics of water-rock interaction of geothermal water

Both sandstone geothermal water and karst geothermal water are different from the closed and open hydrological environment according to chemical composition, mineral water saturation index, coefficient of sodium chloride, desulfurization coefficient, coefficient of salinization, the proportion of ^{14}C age and shell source helium indicators. This is typically due to fracture tectonic activities and relative water thermal storage aquifer weak permeable layer docking. In the closed hydrological environment, the geothermal water stays in the aquifer for a longer time, the water-rock interaction is more complete, the dissolved soluble minerals are more, the concentration is higher, and the renewable capacity of geothermal water is weaker. The excess parameter d value of ^{2}H indicates that karst geothermal water has faster runoff speed and stronger renewable capacity, which is still consistent with the flow characteristics of shallow karst groundwater and sandstone groundwater.

4.3. Source of the geothermal water

Although the karst geothermal water in the eastern part of the Liaokao fault has better runoff conditions and more renewable capacity than the sandstone geothermal water in the western part of the fault, the ^{14}C value of the karst geothermal water is obviously higher than that of the sandstone geothermal water. Because there are Liaokao large fault and its secondary faults and other large faults. The karst geothermal water circulates along the fault to the deep part and obtains the material of higher age in the deep part, while the phenomenon of sandstone geothermal bathymetric circulation convection is very weak or does not exist. Moreover, the closer the fracture is, the higher the proportion of shell source helium and the greater the influence of karst geothermal water on deep materials, indicating that the larger the fracture scale is and the greater the drop is, the more likely it is to lead to upwelling of deep materials.

This further indicates that the sandstone geothermal water in the region is mainly a conducting geothermal system formed by stratified heat storage and lateral runoff recharge. However the karst geothermal water, on the other hand, is stratified heat storage, mainly supplied by lateral runoff, and has deep circulation convection in the larger fault zone, belonging to the conduction and convection geothermal system.

5. Conclusions

(i) The different hydrochemical characteristics of geothermal water indicates that there is no obvious hydraulic connection between the karst geothermal water on the east side of the Liaokao fault and the sandstone geothermal water on the west side.

(ii) The different hydrochemical characteristics of geothermal water of Liaokao fault, indicates that there are obvious zonal differences. And the difference in hydrological environment and water-rock interaction characteristics of the geothermal water in the study area, which is caused by the connection between the thermal reservoir aquifer and the relatively weak permeable layer due to the fault tectonic activity. In the closed hydrological environment, the geothermal water stays in the aquifer for a longer time, the water-rock interaction is more complete, the dissolved soluble minerals are more, the concentration is higher, and the renewable capacity of geothermal water is weaker.

(iii) There is no hot mantle source fluid mixed in the geothermal water in the study area. However, the exist of the Liaokao large fault and its secondary faults, making karst geothermal water circulates along the fault to the deep part and obtains deep crust fluid, while the phenomenon of sandstone geothermal bathymetric circulation convection is very weaker. Moreover, the closer the fracture is, the higher the proportion of shell source helium and the greater the influence of karst geothermal water on deep materials. It is further indicated that the geothermal water in the upper sandstone is mainly stratified conductive geothermal system. Karst geothermal water belongs to layered conduction and zonal convection geothermal system.

Acknowledgements

This research was financially supported by China Geological Survey Project (DD20189114, DD20190129) and the Basic Scientific Research Project of the Chinese Academy of Geological Sciences (JKY1722, YWF201903-01 and JYYWF20180501). The editor, associate editor and anonymous reviewers are thanked for their constructive comments that helped greatly improve the paper.

References

Chen ZH, Wang SN, Wang L, Zha M. 2012. Characteristics of formation water chemical fields and its petroleum significance of the Neogene in Dongying Sag, Shandong Province. Journal of Palaeogeography (Chinese Edition), 14(5), 685–693.

Craig H. 1961. Isotopic variations in meteoric waters. Science, 133(3465), 1702–1703. doi: 10.1126/science.133.3465.1702.

Craig H. 1963. The isotopic geochemistry of water and carbon in geothermal areas. In: Conference on Nuclear Geology in Geothermal Areas. Spoleto, Italy: Consiglio Nationale Delle Recherche Pisa, 17–53.

Du GL, Cao WH, Zhai B. 2012. Genesis of Baoquantang hot spring in Weihai and its influence on faulting and seismic activities. Marine Geology & Quaternary Geology, 32(5), 67–72 (in Chinese with English abstract).

Feng YF, Zhang XX, Zhang B, Liu JT, Wang YJ, Jia DL, Hao LR, Kong ZY. 2018. The geothermal formation mechanism in the Gonghe Basin: Discussion and analysis from the geological background. China Geology, 1, 331–345. doi: 10.31035/cg2018043.

Giggenbach WF, Minissale AA, Scandiffio G. 1988. Isotopic and chemical assessment of geothermal potential of the colli albani area, latium region, Italy. Applied Geochemistry, 3(5), 475–486.

Liu J, Shi J, Yao X, Li Q, Chang ZY. 2018. The control of neo-tectonic activity over geothermal resource in the Taxkorgan Basin on the northeastern margin of the Pamir. Geology in China, 45(4), 681–692 (in Chinese with English abstract).

Luo L, Pang ZH, Luo J, Li YM, Kong YL, Pang JM, Wang YC. 2014. Noble gas isotopes to determine the depth of the geothermal fluid circulation. Chinese Journal of Geology, 49(3), 888–898 (in Chinese with English abstract).

Ma ZY, Qian H. 2004. Environmental Isotope Groundwater Literature. Xi 'an: Shaanxi Science and Technology Publishing House (in Chinese).

Ma ZY, Yu J, Li Q, et al. 2008. Environmental isotope distribution and hydrologic geologic sense of Guanzhong basin geothermal water. Journal of Earth Sciences and Environment, 30(4), 396–401.

Muffler LJP. 1976. Tetonic and hydrologic control of the nature and distribution of geothermal resources. In: Proc. Second U.N. Symposium on the development and use of geothermal resources. San Francisco, 499–507.

Pang ZH, Kong YL, Pang JM, Hu SB, Wang JY. 2017. Geothermal Resources and Development in Xiongan New Area. Bulletin of Chinese Academy of Sciences, (11), 56–62.

Rosberg JE, Erlström M. 2019. Evaluation of the Lund deep geothermal exploration project in the Romeleåsen Fault Zone, South Sweden: A case study. Geothermal Energy, 7(1), 10. doi: 10.1186/s40517-019-0126-7.

Stuart FM, Burnard PG, Taylor RP. 1995. Resolving mantle andcrustal contributions to ancient hydrothermalfluids: He-Arisotopes in fluid inclusions from Dae Hwa W-Mo mineralization, South Korea. Geochim. Cosmochim. Acta, 59(22), 4663–4673.

Sun ZX, Gao B, Zhang ZS. 2014. Isotopic and geochemical evidence for origin of geothermal gases from hotsprings in southern Jiangxi Province, SE-Chine. Chinese Journal of Geology, 49(3), 791–798 (in Chinese with English abstract).

Tang XC, Zhang J, Pang ZH, Hu SB, Wu Y, Bao SJ. 2017. Distribution and genesis of the eastern Tibetan Plateau geothermal belt, western China. Environ Earth Sci, 76, 433–448. doi: 10.1007/s12665-017-6753-z.

Tian TS, Li ML, Bai Y. 2006. Geothermal resources and their development and utilization in China. Beijing: China Environmental Science Press, 7–103 (in Chinese).

Violay M, Heap MJ, Acosta M, Madonna C. 2017. Porosity evolution at the brittle-ductile transition in the continental crust: Implications for deep hydro-geothermal circulation. Scientific Reports, 7(1), 7705. doi: 10.1038/s41598-017-08108-5.

Wang GL, Zhang W, Ma F, Lin WJ, Liang JY, Zhu X. 2018. Overview on hydrothermal and hot dry rock researches in China. China Geology, 1, 273–285. doi: 10.31035/cg2018021.

Wang MJ, He DF, Li WT, Lu RQ, Gui BL. 2011. Geometry, formation evolution and mechanism of Lanliao fault: The boundary of eastern Linqing depression, Bohaiwan Gulf. Chinese Journal of Geology, 46(3), 775–786 (in Chinese with English abstract).

Wang XC, Xiang HF. 2001. Comprehensive study of Liaocheng-Lankao fault and stability analysis of the lower Yellow River. Zhengzhou: Yellow River Water Conservancy Publishing House, 32 –34 (in Chinese).

Xu P, Tan HB, Zhang YF, Zhang WJ. 2018. Geochemical characteristics and source mechanism of geothermal water in Tethys Himalaya belt. Geology in China, 45(6), 1142–1154 (in Chinese with English abstract).

Yang LZ, Zhang GH, Hu NS, Liu CH, Liu ZY. 2009. Recognition of ground water supplying features for northern Shandong plain, China using environmental isotope information. Geological Bulletin of China, 28(4), 515–522 (in Chinese with English abstract).

Yu J, Zhang YL, Wang WZ, Li ZH, Cao WG, Wang LJ. 2013. The evidence of groundwater temperature for Xishanzui buried fault. Journal of Arid Land Resources and Environment, 27(6), 35–40 (in Chinese with English abstract).

Zhang BJ, Shen ZL, Qiao ZB, Qi L. 2009. Analysis on hydro-chemical features and origin of the hot spring in karst geothermal field，east Liaocheng city. Carsologica Sinica, 28(3), 263–268 (in Chinese with English abstract).

Zhang BJ, Shen ZL, Qiao ZB, Qi L. 2010. Hydrochem is trymaterial of underground hot water application in fault determination-Taking geothermal field in Liaocheng city as an example. Geotechnical Investigation & Surveying, 38(1), 51–54 (in Chinese with English abstract).

Zhang BJ, Wen DG, Shen ZL, Qi L. 2009. Geothermal resource of structural trap type: An important geothermal resource conceptual model. Geology in China, 36(4), 927–931 (in Chinese with English abstract).

Zhang Y, Feng JY, He ZL, Li PW. 2017. Classification of geothermal systems and their formation key factors. Earth Science Frontiers, 24(3), 190–198 (in Chinese with English abstract).

Zhao YJ, Liu LJ, Zhang SC, Niu SY, Xia S, Wang M, Wang YH. 2016. Control of Faults on the Geothermal Field Formed. China 's Manganese Industry, 34(4), 29–31 (in Chinese with English abstract).